#### **Research Article**

Jian Yang, Yuqiang Jiang, Weihua Chen, Hui Pan\*, Xing Yang, Miao Li, Tao Liu, Zhanlei Wang, and Yifan Gu

# Paleoenvironmental characteristics of continental shale and its significance to organic matter enrichment: Taking the fifth member of Xujiahe Formation in Tianfu area of Sichuan Basin as an example

https://doi.org/10.1515/geo-2025-0860 received April 21, 2025; accepted July 19, 2025

**Abstract:** Lake-phase organic-rich shales are widely developed in the fifth member (Xu5 Member) of the Triassic Xujiahe Formation in the Sichuan Basin. However, due to the lack of understanding of the paleoclimate and paleoenvironment, the mechanism of organic matter enrichment in the Xu5 Member shale is controversial. To address these issues, this study takes the X5 Member in the Tianfu area as a case study. By analyzing its paleoenvironmental characteristics and correlating with organic matter development, we elucidate the influence of paleoenvironmental conditions on organic matter enrichment patterns in X5 shale. The results show that: (1) the shale of the Xu5 Member has high total organic carbon content and the organic matter type is dominated by type III, which has good potential for anger. (2) Chemical index of alteration (CIA)-weathering index of Parker (WIP) cross-plots indicate first-cycle deposition of the Xu5 Member shales with significant terrigenous input. La/Th, Hf, and Al<sub>2</sub>O<sub>3</sub>/TiO<sub>2</sub> ratios collectively suggest relatively slow sedimentation rates. Provenance analysis reveals dominant felsic igneous sources with minor mafic contributions. C-values and Sr/Cu ratios consistently indicate semi-humid to humid paleoclimatic conditions during deposition. Sr/Ba (<0.5) and Al<sub>2</sub>O<sub>3</sub>/MgO (>7) ratios constrain paleosalinity to freshwater-brackish conditions. Redox proxies (Ni/Co, U/Th, V/Cr, UEF, MoEF) uniformly demonstrate oxygenated bottom-water conditions. Productivity indicators (P/Ti, Cu/Ti, Babio) reveal elevated paleoproductivity in early Xu5<sup>3</sup> to Xu5<sup>2</sup>, with lower values in overlying intervals. (3) The organic matter enrichment of the shale in the Xu5 Member is mainly affected by the redox conditions of the bottom water, paleoproductivity, and paleosalinity, and the more reducing the bottom water is, the higher the paleoproductivity and the higher the paleosalinity are, the more favorable the organic matter enrichment is. In addition, in the sub-member of Xu5<sup>1</sup> and Xu5<sup>2</sup>, paleoclimate, land-source input, and sedimentation rate are also secondary factors affecting the degree of organic matter enrichment.

**Keywords:** Sichuan Basin, terrestrial shale, paleoclimate, paleoproductivity, paleoredox conditions, organic matter enrichment

Jian Yang, Weihua Chen: Research Institute of Engineering Technology, PetroChina Southwest Oil & Gas field Company, Chengdu, 610000, China Yuqiang Jiang, Miao Li, Zhanlei Wang, Yifan Gu: School of Geoscience and Technology, Southwest Petroleum University, Chengdu, 610000, China

Xing Yang: PetroChina Southwest Oil & Gas field Company, Chengdu, 610000. China

**Tao Liu:** Tight Oil and Gas Exploration and Development Project Department of PetroChina Southwest Oil and Gas Filed Company, Chengdu, 610051, China

# 1 Introduction

As one of the unconventional oil and gas reservoirs, the terrestrial organic-rich shale is distributed in major basins around the world and has been proven to have rich oil and gas resources and exploration potential [1–4], including the Triassic Yanchang Formation in the Ordos Basin [5,6], the Permian Lucaogou Formation in the Santanghu Basin [7,8], the Triassic Xujiahe Formation in the Sichuan Basin, and the Jurassic Dongyuemiao Formation [9–12]. At the same time, shale, as one of the main types of fine-grained sedimentary rocks, contains a complete sedimentary record of the

<sup>\*</sup> Corresponding author: Hui Pan, School of Geoscience and Technology, Southwest Petroleum University, Chengdu, 610000, China, e-mail: 1650036990@qq.com

geological period. Because of its overall compactness, it is not easy to receive external fluid interference. Some elements in shale can completely inherit the characteristics of the source rock. Therefore, it is of great significance to analyze the paleoenvironmental conditions of the sedimentary period and its influence on the enrichment of organic matter [13–16]. Due to the frequent changes of climatic conditions, terrigenous input and water properties in the continental sedimentary environment, the paleoenvironmental conditions, rock types, and organic matter enrichment degree in the continental shale sedimentary period have strong heterogeneity in the vertical direction, and the influencing factors of organic matter enrichment are more complex, which brings great challenges to the efficient exploration and development of oil and gas resources [17–20].

Extensive research has been conducted on shale paleoenvironment reconstruction, encompassing key parameters such as paleoclimate, paleosalinity, paleobathymetry, bottom-water redox conditions, paleoproductivity, terrigenous detrital input, and sedimentation rate. These studies have yielded substantial findings and established numerous robust evaluation proxies [21-23]. The influence of paleoenvironmental conditions on organic matter enrichment in shale, particularly continental shale, remains a subject of ongoing debate. One school of thought attributes organic matter (OM) enrichment primarily to individual controlling factors, notably paleoproductivity and bottom-water redox conditions. Conversely, another perspective maintains that OM accumulation results from the interplay of multiple factors, with their relative contributions varying across different depositional stages [24-28]. Furthermore, variations in shale provenance, sedimentary setting, and regional tectonic features contribute to differential paleoenvironmental controls on OM enrichment. Consequently, an integrated assessment incorporating multiple paleoenvironmental parameters is essential for comprehensively evaluating their collective impact on shale OM accumulation [29-31].

However, rapid paleo-water condition fluctuations during deposition – driven by sedimentary environment dynamics – led to frequent shale-siltstone interbedding. This heterogeneity resulted in spatially variable organic matter enrichment across sub-members, whose governing mechanisms remain poorly constrained [32]. Understanding the key controls on organic matter enrichment is critical for optimizing the exploration and development of continental shale gas reservoirs. In this paper, the fifth member of the Xujiahe Formation in the Tianfu area of the central Sichuan Basin is taken as the research object. Based on the intensive coring data of the fifth member of Xujiahe Formation in Well YQ1, the major elements, trace elements, rare earth elements, and organic geochemical analysis of the fifth member of Xujiahe Formation shale are carried out. The organic matter content of the fifth member of

Xujiahe Formation shale and the characteristics of paleoclimate, paleoweathering conditions, paleosalinity, paleoredox conditions, and paleoproductivity during the sedimentary period are clarified, and the main controlling factors of organic matter enrichment in each sub-member are discussed in order to provide reference for the accumulation mechanism of shale gas in Xujiahe Formation of Sichuan Basin.

# 2 Geological overview

The Sichuan Basin is located in the southwest of China. It is a first-order tectonic unit of the Yangtze stable platform. The north is the Micangshan and Dabashan fold belt, the northwest is the Longmenshan fold belt, the south is the Emeishan-Washan fold belt and Laoshan fold belt, and the east is the Sichuan-Hunan fold belt (Figure 1a) [33-35]. The Sichuan Basin mainly developed marine sedimentary strata in the Early Triassic and before. Under the influence of the Indo-Chinese movement in the Middle Triassic, the basin as a whole uplifted, and the seawater gradually withdrew from the basin, gradually changing from marine deposits to continental deposits. During the sedimentary period of the Xujiahe Formation, the river-delta-lake sedimentary system was widely developed in the basin, forming a set of clastic rock deposits of sand-mudstone interbeds. Since the late Triassic, the Sichuan Basin has been affected by the multidirectional compression of the periphery, ending the evolution stage of the passive continental margin and forming a series of foreland basins and paleo-uplift slopes [36,37].

The Tianfu area is located in the western part of the low fold belt in central Sichuan and the slope belt in the eastern part of the western Sichuan depression. Under the influence of the foreland basin, the formation of the Xujiahe Formation is gradually thinning from west to east, which is divided into six members. Among them, the first, third, and fifth members of Xujiahe Formation are mainly lake and swamp facies sedimentary environment. The lithology is mainly gray black shale and silty mudstone, with a small amount of thin coal line and siltstone, which is the main source rock of the Xujiahe Formation [38,39]. The second, fourth, and sixth members of the Xujiahe Formation are mainly delta facies deposits. The lithology is mainly thick gray-white sandstone, with a small amount of gray-black mudstone, which is the main reservoir member of the Xujiahe Formation [33,40,41]. The target layer of this study is the fifth member of the Xujiahe Formation. The overall thickness is large and can be divided into four sub-members. The thickness of each sub-member is between 54 and 119, and the formation thickness is relatively close.

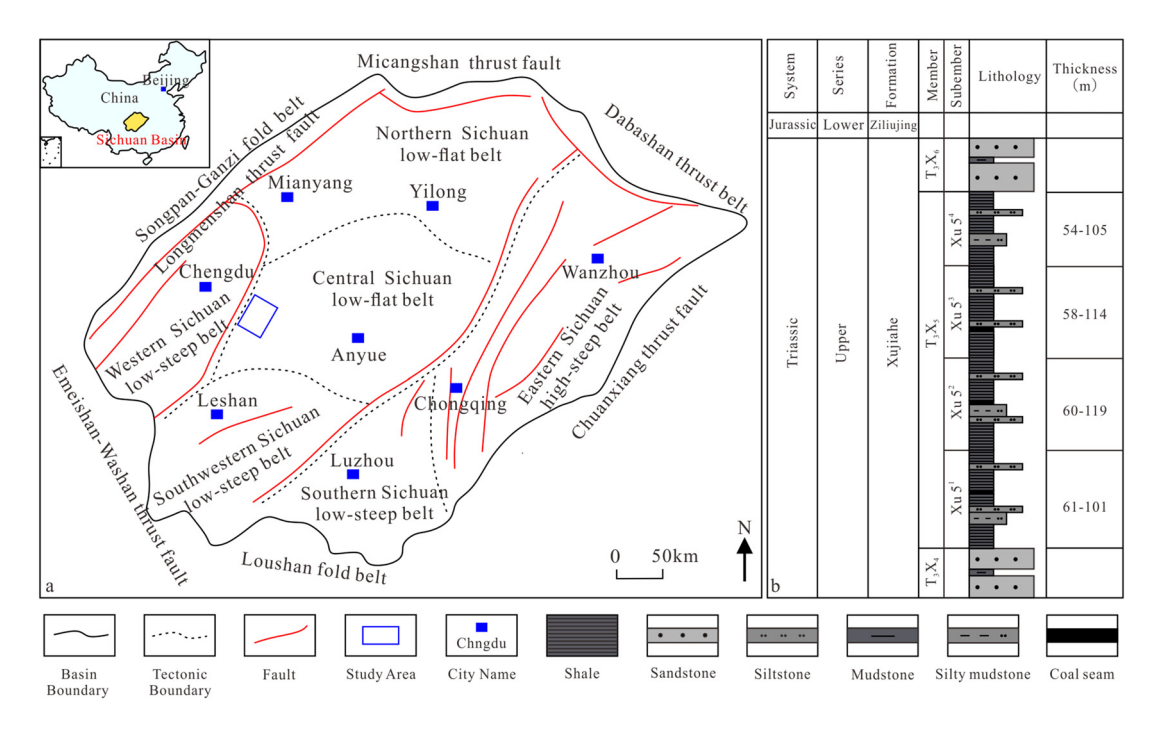


Figure 1: The structural position of the study area and the histogram of the fifth member of the Xujiahe Formation. (a) Structural location of the study area and (b) columnar diagram of the fifth member of Xujiahe Formation in the study area.

# 3 Sample information and experimental methods

# 3.1 Sample information

The samples of this study are from the YQI well, and the sampling depth is between 3,048 and 3,576 m. A total of 67 samples were taken, including 18 in the fifth member, 16 in the second member, 15 in the third member, and 18 in the fourth member. These samples are mainly gray-black and black shale and contain a small amount of silty mudstone. All samples were measured for total organic carbon (TOC) content and whole-rock elements. Thirty-five samples were selected for rock pyrolysis analysis and whole rock and clay X-ray diffraction (XRD) analysis.

#### 3.2 Experimental method

#### 3.2.1 TOC

Before TOC determination, the sample needs to be ground into powder with a diameter greater than 200 mesh, and 12.5% hydrochloric acid solution is used to fully react with the sample to achieve the purpose of eliminating carbonate minerals in the sample. Then the sample powder is dried, and the dried sample is placed in an oven at 1,350°C for combustion, and the organic carbon content is determined by the CO<sub>2</sub> generated by the infrared detector [23,24].

#### 3.2.2 Whole-rock element determination

The content of major elements in the samples was measured by X-ray fluorescence (XRF) spectrometry. First, the sample was made into a powder with a diameter of less than 200 mesh and dried for 12 h. Then the dried sample powder was heated at 1,000°C for 2 h. After the sample was cooled to 400°C, the weight loss of the sample was weighed and recorded. Finally, the sample was mixed with lithium tateborate (Li<sub>2</sub>B<sub>4</sub>O<sub>7</sub>) and melted into glass beads for XRF elemental analysis. For the analysis of trace elements and rare earth elements (REEs), powder samples were also used. First, the sample powder was treated with a highpressure polytetrafluoroethylene bomb in HF and HNO3 solutions, and the sample was heated to 150°C and dried for 12 h, followed by inductively coupled plasma mass spectrometry (ICP-MS) [26-28].

#### 3.2.3 Rock pyrolysis analysis

The sample pretreatment method of rock pyrolysis analysis is consistent with the TOC determination. The OGE-VI hydrocarbon evaluation workstation instrument is used to pyrolyze the rock, and then the flame ionization detector and the thermal conductivity detector are used to detect the H2 and  $\rm CO_2$  gases released by the organic matter after heating. The measured parameters include free hydrocarbon content (S1), pyrolysis hydrocarbon content (S2), S2 maximum temperature peak ( $T_{\rm max}$ ), and hydrogen index (HI) [43,44].

#### 3.2.4 XRD

In the XRD experiment, the powder sample with a diameter of less than 200 mesh was used for determination. First, the sample was heated to 150°C for drying for 12 h, and then, the content of various minerals in the sample was analyzed by "D8A" X-ray diffractometer [20,21].

#### 3.3 Index calculation method

The paleoclimate and paleoweathering conditions are characterized by paleoclimate index C, chemical alteration index CIA, component variation index ICV, and weathering index WIP [42–45]. The specific calculation formulas are as follows:

$$C - \text{value} = \sum (\text{Fe} + \text{Mn} + \text{Cr} + \text{Ni} + \text{V} + \text{Co}) / \sum (\text{Ca} + \text{Mg} + \text{Sr} + \text{Ba} + \text{K} + \text{Na}),$$
(1)

CIA = 
$$[Al_2O_3/(Al_2O_3 + CaO* + Na_2 O + K_2O)] \times 100\%$$
, (2)

ICV = 
$$(Fe_2O_3 + K_2 O + Na_2 O + CaO * + MgO + MnO + TiO_2)/Al_2O_3$$
, (3)

WIP = 
$$(CaO*/0.7 + 2Na_2O/0.35 + 2K_2O/0.25 + MgO/0.9)$$
  
× 100%.

All the oxides are molar mass, and CaO\* is the molar content of CaO in silicate. The CaO in apatite is corrected by P2O5 data (CaO' = CaO-10/3  $\times$  P<sub>2</sub>O<sub>5</sub>), and then, the molar number of CaO' and Na<sub>2</sub>O is compared. The value of CaO\* is the smaller value between CaO' and Na<sub>2</sub>O.

The enrichment factor XEF is usually used to indicate the degree of enrichment of elements and can be used to eliminate the influence of terrestrial debris. It can be calculated using the following formula:

$$XEF = (X/Al)sample/(X/Al)UCC.$$
 (5)

In the formula, X is the concentration of elements and the upper continental crust (UCC) standard is selected from Wedepohl [46]. The biological Ba ( $Ba_{bio}$ ) is usually used to determine the paleoproductivity of the sedimentary period [47], and its calculation formula is

Babio = 
$$Ba_{sample} - Al_{sample} \times (Ba/Al)_{paas}$$
. (6)

# 4 Results

## 4.1 Petrological characteristics

According to the mineral content obtained by XRD, the lithology classification triangle is drawn. The results show that the shale in the fifth member of Xujiahe Formation is mainly clay shale and felsic shale, containing a small amount of mixed shale (Figure 2a). The content of clay minerals and quartz is high. The content of clay minerals is between 20.3 and 73.7%, with an average of 46.1%. The content of quartz is between 18.9 and 62.9%, with an average of 40.1%. The content of feldspar is between 0 and 11.2%, with an average of 5.7%. The content of carbonate minerals is relatively small, with an average of 3.6%. The content of carbonate minerals in individual samples is relatively high. Up to 25.2%. A small amount of siderite is also developed in the shale of the fifth member of the Xujiahe Formation, and its content is between 0 and 6.4%, with an average value of 0.8 (Figure 2b).

#### 4.2 Geochemical characteristics of elements

#### 4.2.1 Major elements

The major elements in the shale of the fifth member of Xujiahe Formation are mainly  $SiO_2$ ,  $Al_2O_3$ , and  $Fe_2O_3$ , with an average content of 52.95, 13.64, and 5.92%, respectively, and the remaining oxides are less. The normalized distribution of major elements in each sub-member of the fifth member of the Xujiahe Formation using UCC is shown in Figure 3b. Compared with UCC, most of the major elements in each sub-member of the fifth member of the Xujiahe Formation are relatively enriched, among which  $P_2O_5$  is highly enriched, and the enrichment degree is the highest in the third sub-member of the fifth member of the Xujiahe Formation, which may be related to the higher paleoproductivity during this period. The content of  $Na_2O$  in each sub-member is significantly lower than that of UCC, indicating that the content of plagioclase in the parent rock

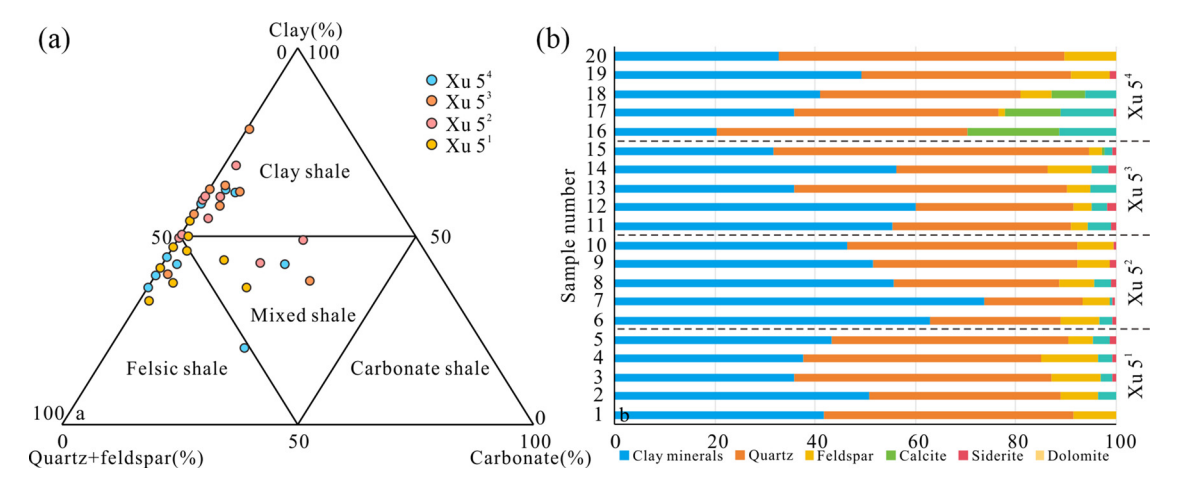
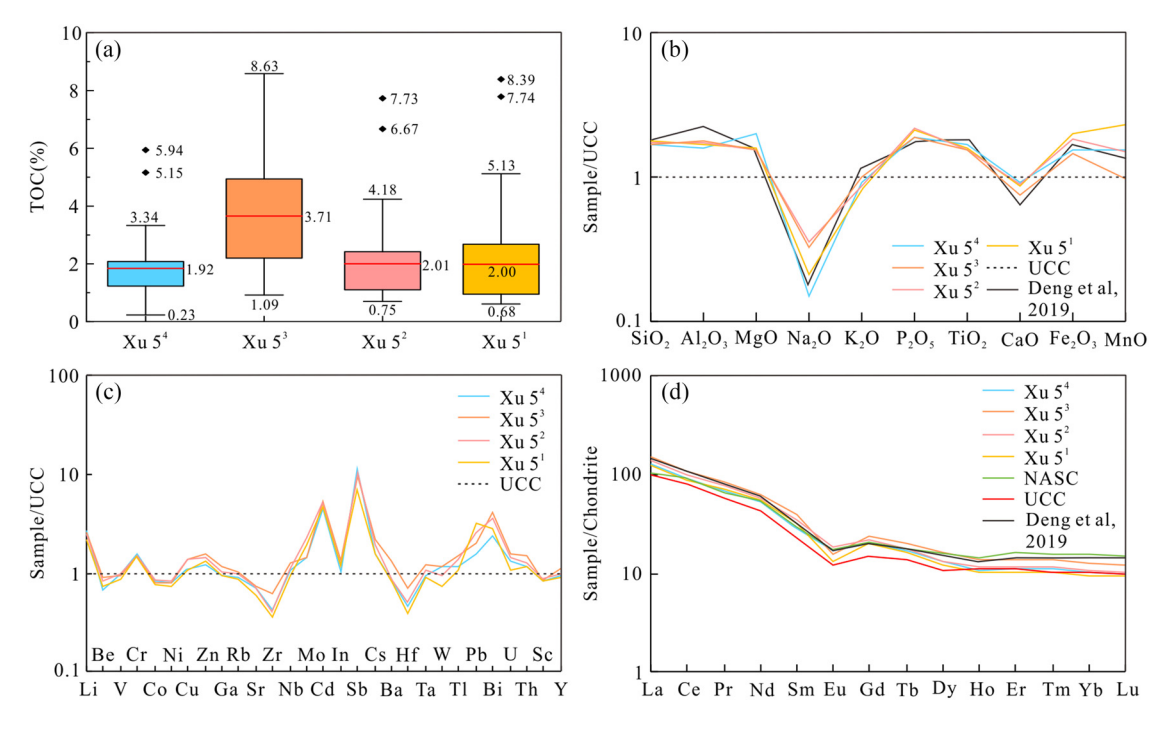


Figure 2: Shale lithology classification triangle (a) and mineral content distribution of some samples (b).

is low and the source may come from acidic magmatic rocks. The content of CaO is generally low, showing a weak negative anomaly compared with UCC, which is related to the low content of carbonate minerals in the shale of the fifth member of the Xujiahe Formation. There are some differences in the enrichment degree of the Mn element in each sub-member. The overall performance is that the content of the Mn element gradually increases from  ${\rm Xu5}^1$  to  ${\rm Xu5}^3$  sub-member, and gradually decreases to  ${\rm Xu5}^4$  sub-member.

#### 4.2.2 Trace elements

Figure 4c presents the UCC-normalized trace element distribution patterns. The sub-members exhibit consistent distribution trends with minor amplitude variations in localized intervals, suggesting relatively stable provenance conditions during deposition of the Xu5 Member. Most elements (e.g., Be, V, Rb, Ba) cluster around the UCC reference line (value = 1). Distinct geochemical fractionation is observed: Li, Cd, Sb, Pb, and Bi display significant



**Figure 3:** TOC and element distribution characteristics of each sub-member of the fifth member of the Xujiahe Formation. (a) TOC distribution box diagram; (b) UCC standardized distribution map of major elements; (c) UCC standardized trace element distribution map; and (d) crystal normalized REE distribution map.

6 — Jian Yang et al. DE GRUYTER

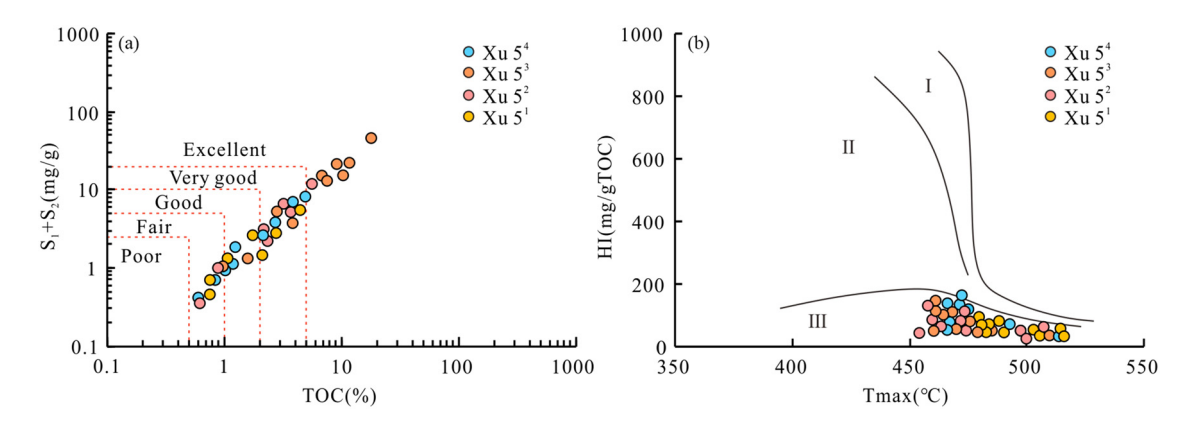


Figure 4: Organic geochemical characteristics of the fifth member of the Xujiahe Formation shale. (a) TOC – S1 + S2 crossplot and (b) HI –  $T_{max}$ .

enrichment relative to UCC, whereas Zr, Sr, and Hf show marked depletion (Figure 3c).

#### 4.2.3 REEs

Figure 3c displays chondrite-normalized REE distribution patterns. Shale samples from all sub-members of the Xujiahe Formation Member 5 exhibit consistent REE signatures: (1) light REE (LREE) enrichment, (2) flat heavy REE (HREE) patterns, and (3) weak negative Eu anomalies. These characteristics show remarkable similarity to both UCC and North American Shale Composite (NASC) patterns [48,49]. There are slight differences in the distribution patterns of REEs between the sub-members. These differences may reflect that the provenance and sedimentary process of each sub-member have changed to a certain extent, such as sedimentary water conditions, rock weathering degree, or sediment recycling.

# 4.3 Organic geochemical characteristics

Through the TOC measurement of the shale samples in the fifth member of the Xujiahe Formation, the results show that the overall TOC content of the shale in the fifth member of the Xujiahe Formation is high, but the content of TOC in each sub-member is different (Figure 3a). The TOC content of the third sub-member of the Xujiahe Formation is the highest, mainly distributed in 1.09–8.63%, with an average of 3.71%. The TOC content of the remaining three sub-members is relatively close, which is lower than that of the Xu5<sup>3</sup> sub-member. The TOC of the Xu5<sup>4</sup> sub-member is mainly between 0.23 and 3.34%, with an average of 1.92%. The TOC of the Xu5<sup>2</sup> sub-member is mainly between 0.75 and 4.18%, with an average of 2.01%. The

TOC of the Xu5<sup>1</sup> sub-member is mainly distributed in 0.68 and 5.13%, with an average of 2.01%. The TOC content of individual samples in these three sub-members is high, which can exceed 8% (Figure 3a), which is related to the carbonized plant debris in the sample. According to the discriminant chart of TOC and free hydrocarbon (S1) + pyrolysis hydrocarbon (S2) (Figure 4a), the results show that the organic matter content of the shale is high, and most of the samples have good-very good hydrocarbon generation potential; only a small number of samples have general hydrocarbon generation potential. The rock pyrolysis parameters show that the HI of the shale in the study area is between 0.38 and 198 mg/g TOC, and the maximum temperature peak ( $T_{\text{max}}$ ) of S2 is between 453 and 521°C, with an average value of 480°C. According to the  $HI-T_{max}$  discriminant chart, the organic matter type of the shale in the fifth member of the Xujiahe Formation is mainly type III (Figure 4b), which is consistent with the previous research on the coal-bearing source rocks of the Xujiahe Formation.

# 5 Discussion

#### 5.1 Paleoclimate

The *C*-value is a common indicator for judging the paleoclimate during the sedimentary period. The current research generally believes that Fe, Mn, Cr, Ni, V, and Co are easily enriched under wet conditions, while Ca, Mg, Sr, Ba, K, and Na are enriched under dry conditions. Therefore, *C*-value of 0.8 is a humid climate. The Sr/Cu ratio serves as a robust paleoclimate proxy for the depositional period. Under humid conditions, Cu exhibits higher enrichment affinity, whereas Sr preferentially accumulates

during arid phases. Consequently, elevated Sr/Cu ratios indicate drier paleoclimatic conditions. Usually, when the ratio of Sr/Cu is between 1 and 10, it represents a warm and humid climate, and when the ratio is greater than 10, it represents a dry and hot climate [50,51]. It can be seen from the cross plot of *C*-value and Sr/Cu (Figure 5a) that the *C*-value of the shale in the fifth member of Xujiahe Formation is generally greater than 0.4, and the Sr/Cu ratio of most samples is between 1 and 10, only a few samples are greater than 10, indicating that the paleoclimate of the fifth

member of Xujiahe Formation is generally under relatively humid conditions. These findings align with previous studies of Member 5 of the Xujiahe Formation across the Sichuan Basin, reinforcing the regional consistency of freshwater-brackish depositional environments during this period [9]. At the same time, the *C*-value gradually decreases and the Sr/Cu ratio gradually increases from Xu5<sup>1</sup> to Xu5<sup>4</sup>, indicating that the drought degree of the paleoclimate during the deposition period of Xu5 gradually increases (Figure 7).

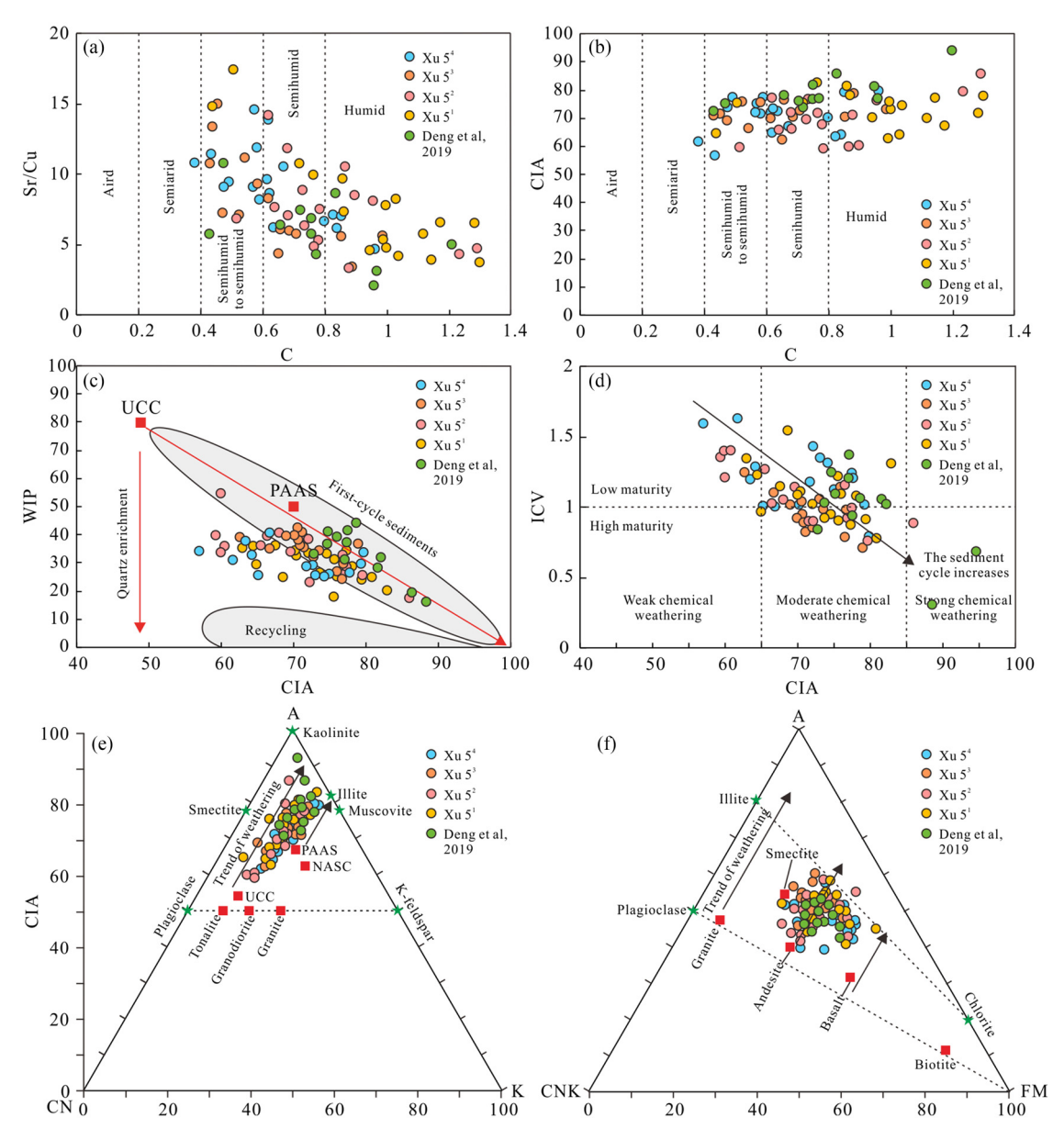


**Figure 5:** The distribution map of paleoclimate parameters and paleoweathering condition parameters in the fifth member of Xujiahe Formation. (a) Crossplot of *C*-value and Sr/Cu ratio; (b) the intermember diagram of *C*-value and CIA value; (c) crossplot of CIA value and WIP value; (d) crossplot of CIA value and ICV value; (e) A-CN-K triangle; and (f) A-CNK-FM.

# 5.2 Paleo-weathering conditions and sedimentary recycling

The CIA is a key geochemical proxy for rock weathering intensity. Elevated CIA values (85-100) indicate intense chemical weathering under warm/humid climates with high precipitation, while values of 65-85 and 50-65 reflect moderate and weak weathering regimes, respectively [52,53]. The CIA index in the shale of the fifth member of the Xujiahe Formation is generally between 60 and 85. indicating a weak-medium chemical weathering intensity, and with the increase of C-value, the CIA value increases slightly (Figure 6b), indicating that as the climate becomes warm and humid, the degree of chemical weathering gradually increases. The WIP provides enhanced sensitivity to quartz dilution effects induced by sedimentary recycling and hydraulic sorting, making it particularly effective for evaluating weathering intensity in mature sediments [45]. The CIA-WIP intermember diagram shows that there is a linear negative correlation between WIP and CIA (Figure 5c), indicating that there is obvious quartz enrichment in the samples of the fifth member of the Xujiahe Formation, which is in the primary sedimentary stage as a whole, and some samples are shifted to the direction of cyclic deposition, indicating the influence of sedimentary sorting on quartz content. The compositional variation index ICV can be used to determine the compositional maturity of clastic rocks, the intensity of weathering, and re-deposition. When ICV > 1, the compositional maturity of the sample is low, indicating that the content of unweathered minerals in the rock is high and tends to be deposited for the first time. The ICV-CIA intermember diagram shows that the ICV values of the samples in the Xu5<sup>4</sup> sub-member are generally greater than 1, which is the first deposition. The ICV values of most samples in the remaining sub-members are greater than 1, and the ICV values of a small number of samples are less than 1, indicating that they may be affected by weak recycling. Consistent with the findings of Deng et al. [9], the comparable CIA, WIP, and ICV values between this study and adjacent areas suggest uniformly weak-to-moderate weathering intensities for the Xu5 Member across the Sichuan Basin. These geochemical signatures support its interpretation as primarily firstcycle deposits.

The  $Al_2O_3$  – (CaO\* + Na<sub>2</sub>O) – K<sub>2</sub>O (A-CN-K) and  $Al_2O_3$  – (CaO\* + Na<sub>2</sub>O + K<sub>2</sub>O) – (Fe<sub>2</sub>O<sub>3</sub> + MgO) (A-CNK-FM) triangle diagrams can also be used to analyze the weathering intensity of rocks. In the A-CN-K triangle diagram (Figure 5e), the predicted chemical weathering trend is parallel to the A-CN change and approximately parallel to the trend of sample

distribution, indicating that the metasomatism of potassium has no obvious effect on the sample. The intermediate weathering stage is marked by illite. The sample plots between the UCC and illite compositional endmembers, suggesting an intermediate weathering stage characteristic of illite formation. The A-CNK-FM ternary diagram (Figure 5f) shows sample compositions plotting between the plagioclase-FM join and the chlorite-illite trend line, further confirming moderate chemical weathering in the Xujiahe Formation Member 5 shales. Integrated analysis suggests these shales represent primarily first-cycle deposits with minor recycled components. There is no significant change in the CIA index from the first sub-member of the fifth member to the fourth sub-member of the fifth member. The weathering is generally moderate chemical weathering. The ICV index shows a high value in the early stage of the second sub-member of the fifth member and the sedimentary period of the fifth member of the fifth member, and the composition maturity of the rock is high (Figure 6).

# 5.3 Paleosalinity

The salinity of the water during the deposition period has an important influence on the formation of source rocks and the preservation of organic matter. Previous studies have shown that the Sr/Ba ratio has a good effect on the reconstruction of the paleosalinity of the sedimentary water, and the Sr/Ba ratio 1 represents the saline water environment. The content and variation of Mg and Al elements are also one of the reliable indicators to indicate the paleosalinity of sedimentary water. The ratio of Al<sub>2</sub>O<sub>3</sub>/MgO greater than 7 indicates the freshwater environment, and the ratio of Al<sub>2</sub>O<sub>3</sub>/MgO less than 7 indicates the saline water environment [54,55]. The Sr/Ba and C-value crossplot (Figure 7a) reveals Sr/Ba ratios predominantly <1, suggesting freshwater to brackish conditions in the Xu5 Member. While paleoclimate typically influences salinity through evaporative concentration in arid settings, the lack of correlation and scattered distribution of elevated Sr/Ba ratios across climate regimes indicate paleoclimate exerted secondary control on paleosalinity relative to other factors. The crossplot of Al<sub>2</sub>O<sub>3</sub> content and MgO content (Figure 7b) shows that the Al<sub>2</sub>O<sub>3</sub>/MgO ratio of the Xu5 samples is generally greater than 7, which also indicates that the water body salinity is low during the sedimentary period, which is a freshwater environment. Consistent with previous studies, the diagnostic geochemical

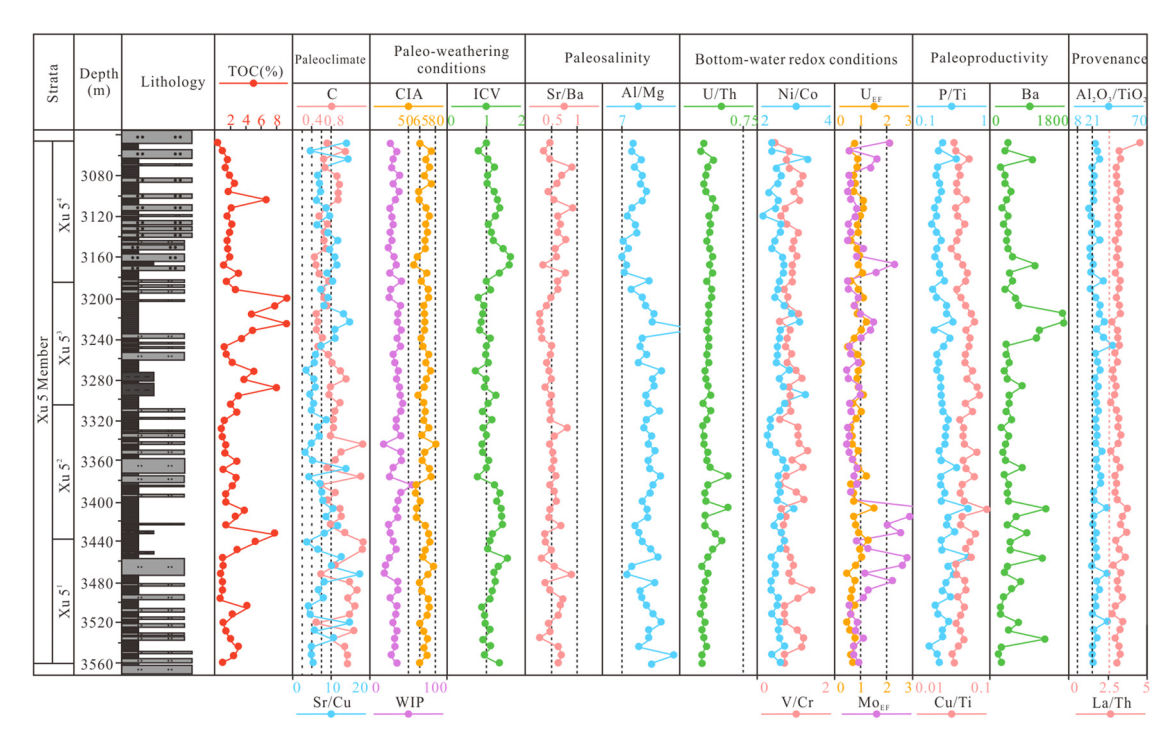


Figure 6: Vertical variation of TOC and paleoenvironmental indicators in the fifth member of Xujiahe Formation in Well YQ1.

signatures (Sr/Ba < 0.5 and  $Al_2O_3/MgO > 7$ ) observed in this study confirm a low-salinity freshwater depositional environment for the Xujiahe Formation (Figure 7a) [9]. These ratios collectively reflect minimal marine influence and predominant terrestrial freshwater conditions during sedimentation. On the whole, the Sr/Ba ratio is generally distributed between 0 and 0.5 or close to 0.5, the  $Al_2O_3/MgO$  ratio is generally high, and the paleosalinity of the water body is reduced. The Sr/Ba increased significantly and the  $Al_2O_3/MgO$  ratio decreased in the sub-members from  $Xu5^4$ , which represented the gradual increase of salinity and the gradual transition from fresh water to brackish water (Figure 6).

#### 5.4 Paleo-redox conditions

Paleo-redox conditions of the water column during deposition exerted fundamental control on organic matter preservation in sediments. Redox-sensitive trace elements (Mo, V, U) exhibit valence-state-dependent mobility, making them particularly sensitive proxies for reconstructing water redox conditions. Ni element mainly exists in the form of soluble Ni<sup>2</sup> ion in the oxidation environment, while it is insoluble in water under the reduction condition. Therefore, it can usually be distinguished by Ni/Co ratio, U/Th ratio, V/Cr ratio and enrichment factor (EF)

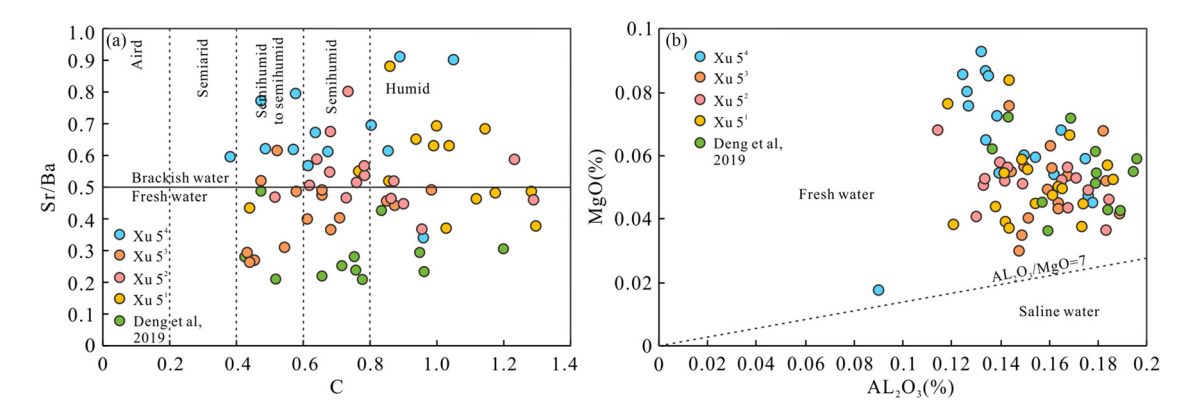
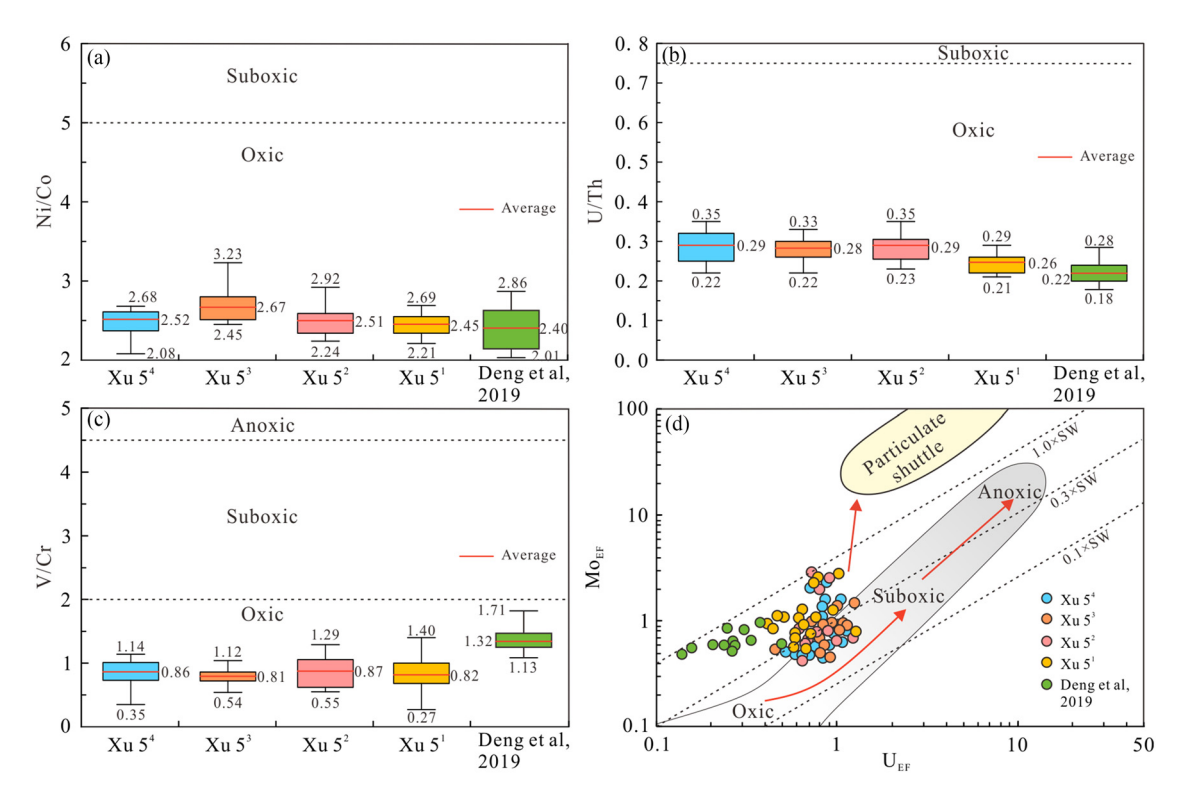


Figure 7: The paleosalinity discrimination diagram of the fifth member of the Xujiahe Formation. (a) Sr/Ba-C content crossplot and (b)  $Al_2O-MgO$  content crossplot.

10 — Jian Yang et al. DE GRUYTER



**Figure 8:** Discriminant diagram of ancient redox conditions in Xu5 member. (a) The distribution map of Ni/Co ratio; (b) U/Th ratio distribution map; (c) V/Cr ratio distribution map; and (d) the intermember diagram of U<sub>FF</sub> and Mo<sub>FF</sub>.

of U and Mo [56,57]. According to previous studies, Ni/Co ratio < 5, U/Th ratio < 0.75, V/Cr ratio < 2 represent oxygenrich environment, Ni/Co ratio between 5 and 7, U/Th ratio between 0.75 and 1.25, V/Cr ratio between 2 and 4.5 represent hypoxic environment, Ni/Co ratio > 7, U/Th ratio > 1.25, V/Cr ratio > 4.5 represent hypoxic environment, the higher the enrichment degree of U and Mo, the lower the oxygen content in the water [58,59]. The statistical results show that the Ni/Co ratio of the samples in the fifth member of Xujiahe Formation is generally less than 5, the maximum

value is 3.23 (Figure 8a), the U/Th ratio is less than 0.75, the maximum value is 0.35 (Figure 8b), and the V/Cr ratio is less than 2, the maximum value is 1.40 (Figure 8c), indicating that the water body during the deposition period of the fifth member of Xujiahe Formation was in an oxygenrich environment. There was no significant difference in the ratios of various types of samples in each sub-member, and the oxidation-reduction conditions of the bottom water were basically the same. The intermember diagram of  $Mo_{EF}$  and  $Mo_{EF}$  shows that  $Mo_{EF}$  is mainly distributed in

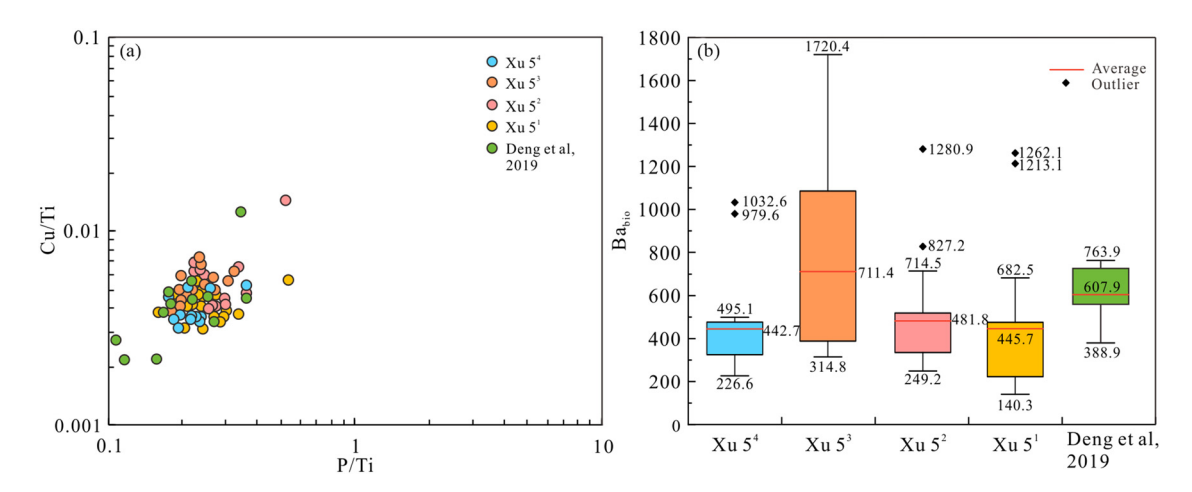


**Figure 9:** The distribution map of paleoproductivity index in the fifth member of Xujiahe Formation. (a) Cu/Ti and P/Ti crossplots and (b) Babio content distribution map.

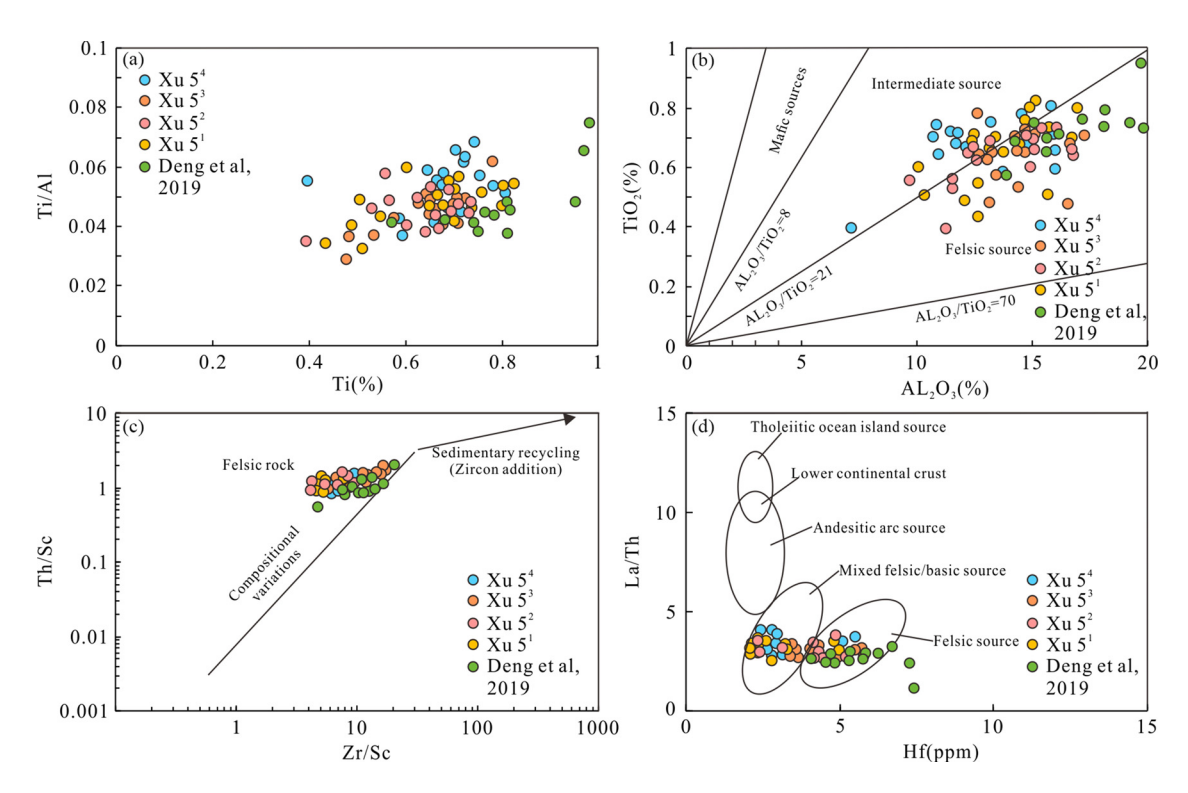


**Figure 10:** Terrestrial clastic input and source rock discrimination diagram of the fifth member of Xujiahe Formation. (a) Ti/Al-Ti content crossplot; (b) Al<sub>2</sub>O<sub>3</sub>-TiO<sub>2</sub> crossplot; (c) Th/Sc-Zr/Sc intermember diagram; and (d) La/Th-Hf cross plot.

0.42-2.86, with an average value of 1.26, and  $U_{EF}$  is mainly distributed in 0.41-1.54, with an average value of 0.79. The overall performance is characterized by relative loss, which also indicates that the oxygen content of the water body during the deposition period is high and the reduction of the bottom water is poor. The Ni/Co and U/Th ratios exhibit comparable ranges to previous studies, while the slightly elevated V/Cr values remain within the oxidative threshold, collectively supporting our interpretation of oxic depositional conditions (Figure 8) [9]. On the whole, the bottom water in the sedimentary period of the fifth member of the Xujiahe Formation is under the condition of oxygen enrichment. From the end of the fifth member of Xujiahe Formation to the early stage of the fifth member of Xujiahe Formation, there is a short-term increase in U/Th ratio and UEF, and the reducibility of bottom water is enhanced, and then the overall oxygen-enriched environment is changed (Figure 6).

# 5.5 Paleoproductivity

Paleoproductivity serves as a fundamental parameter for assessing ancient lacustrine systems, exerting significant control on organic matter formation and accumulation. Among various geochemical proxies, P/Ti and Cu/Ti ratios

have proven particularly reliable for paleoproductivity reconstruction. Phosphorus (P), as a key biolimiting nutrient, directly reflects biological productivity through its sedimentary abundance. Copper (Cu) predominantly associates with organic matter through organometallic complexation, making its content an effective tracer of organic matter flux. At the same time, biological Ba (Babio) usually settles near the interface of water and sediment with organic matter, resulting in local Ba enrichment. Therefore, Babio is also considered as one of the indicators for judging paleoproductivity and is widely used in the discrimination of lake or marine sediments [43,60-62]. The crossplot of P/Ti and Cu/Ti (Figure 9a) shows that the two ratios of the samples in the fifth member of the Xujiahe Formation have the same change trend. The P/Ti ratio is between 0.25 and 0.53, with an average value of 0.16, and the Cu/Ti ratio is between 0.003 and 0.014, with an average value of 0.005, indicating that the shale in the fifth member of the Xujiahe Formation has medium paleoproductivity. The Babio distribution map (Figure 9b) shows that the paleoproductivity level of each sub-member is basically consistent with the TOC distribution characteristics. Among them, the Babio content of the Xu5<sup>3</sup> sub-member is the highest, with an average value of 711.4, and the paleoproductivity is higher. The Babio content of the remaining submembers is relatively close, and the paleoproductivity level is lower than that of the Xu5<sup>3</sup> sub-member. Regional

comparison reveals the study area's paleoproductivity is moderately lower than adjacent Xu5<sup>4</sup>, Xu5<sup>3</sup>, and Xu5<sup>1</sup> submembers, with Xu5<sup>3</sup> exhibiting the highest productivity levels. This spatial variability likely reflects differences in nutrient supply and water column conditions across the paleo-lake. On the whole, Cu/Ti, P/Ti and Babio gradually increased from the middle to the early stage of Xu5<sup>2</sup> submember, representing the gradual increase of paleoproductivity. The paleoproductivity level was low from the middle stage of Xu5<sup>2</sup> sub-member to the middle stage of the Xu5<sup>3</sup> sub-member, and reached the highest level at the end of the Xu5<sup>3</sup> sub-member. The TOC content of shale was also high during this period, and the paleoproductivity of the Xu5<sup>4</sup> sub-member returned to a lower level (Figure 6).

## 5.6 Terrestrial debris input and provenance

Terrigenous detrital input intensity and provenance constitute fundamental attributes of fine-grained sedimentary rocks that can be effectively quantified through geochemical proxies. The terrigenous input flux is typically characterized using Ti and Al concentrations, where elevated Al content indicates enhanced terrigenous contribution, while increased Ti/Al ratios suggest comparatively higher sedimentation rates.[51,63]. The Ti/Al versus Ti bivariate plot (Figure 10a) reveals that samples from the Xujiahe Formation Member 5 exhibit Ti concentrations predominantly ranging from 0.4 to 0.8%, indicative of significant terrigenous detrital input. The strong positive correlation between these parameters demonstrates terrigenous control on sedimentation rates throughout Member 5 deposition. Notably, both sedimentation rates and terrigenous input intensity show progressive upward increases within the member, as evidenced by systematic trends in Ti/Al ratios and absolute Ti contents.

The chemical properties of  $Al_2O_3$  and  $TiO_2$  tend to be inert, and their solubility is usually low in low-temperature liquids. The ratio of  $Al_2O_3$  to  $TiO_2$  in sediments is usually similar to that in parent rocks, so they can be used for provenance analysis of sediments. According to previous studies [64], the  $Al_2O_3/TiO_2$  ratio between 21 and 70 represents the felsic source, the ratio between 8 and 21 represents the medium source, and the ratio between 3 and 8 represents the mafic source. The intermember diagram of  $Al_2O_3$  and  $TiO_2$  (Figure 10b) shows that the  $Al_2O_3/TiO_2$  ratio is between 8 and 70, indicating that the parent rock of the fifth member of the Xujiahe Formation shale comes from felsic source rock and medium source rock. Th and Sc

exhibit minimal geochemical mobility during sedimentary processes, being exclusively transported via terrigenous detrital input, thus serving as reliable provenance indicators. Systematic increases in Th/Sc and Zr/Sc ratios are observed in fine-grained sedimentary rocks transitioning from mafic to felsic source terrains. The Th/Sc–Zr/Sc discrimination diagram (Figure 10c) reveals elevated ratio values for the Xu Member shales, demonstrating derivation from felsic igneous provenances without significant sedimentary recycling. These findings show excellent consistency with provenance interpretations based on  $Al_2O_3/TiO_2$  systematics.

REE fractionation patterns serve as effective proxies for both sedimentary residence time and depositional rates. Under high sedimentation rate conditions, limited aqueous residence time results in (1) reduced LREE/HREE fractionation and (2) concurrent deposition of both element groups. Conversely, low sedimentation rates promote extended suspension durations that enhance LREE-HREE fractionation through differential scavenging processes [65]. At present, the NASC normalized La/Th ratio is generally considered to be a reliable indicator for evaluating the deposition rate of geological periods. The closer the ratio is to 1, the faster the deposition rate is, and the slower the deposition rate will make the ratio away from 1 [66,67]. The statistical results show that the La/Th ratio of the shale samples in the fifth member of the Xujiahe Formation is between 2.64 and 4.92, reflecting the slow deposition rate. The La/Th-Hf crossplot (Figure 10d) shows that the samples of the fifth member of the Xujiahe Formation shale fall in the felsic source rock area and the felsic/mafic source rock mixed area, which is basically consistent with the Al<sub>2</sub>O<sub>3</sub>/ TiO<sub>2</sub> ratio discrimination method and the Th/Sc-Zr/Sc crossplot discrimination chart. In summary, the source of the fifth member of the Xujiahe Formation shale is mainly from the felsic igneous rock and the felsic/basic source rock mixed source rock, and there is no significant change in the Al<sub>2</sub>O<sub>3</sub>/TiO<sub>2</sub> ratio and La/Th ratio from the first submember to the fourth sub-member of the Xujiahe Formation, indicating that the source of each sub-member is basically the same, and the overall deposition rate is relatively slow (Figure 6). While depositional rates align with previous studies, significant provenance differences exist (Figure 10d). Deng et al. [9] western Sichuan study area received predominantly felsic detritus from proximal western sources, whereas our central-western Sichuan slope location shows mixed felsic/mafic signatures due to: (1) longer transport distances allowing greater sediment mixing and (2) contributions from eastern basic provenances. This spatial variation in source rock composition reflects the basin's complex tectonic framework [9].

# 5.7 Main controlling factors of organic matter enrichment

The enrichment of organic matter in continental shale is usually affected by paleoenvironmental characteristics such as paleoclimate, paleosalinity, and paleoproductivity. The organic matter content of each sub-member of the fifth member of the Xujiahe Formation in the study area and the evolution of the paleoenvironment during the sedimentary period were analyzed. On this basis, the main controlling factors of shale organic matter enrichment in each submember were explored by correlation analysis (Figure 11). The analysis results show that the C-value and CIA value are positively correlated with the TOC content (Figure 11a and b), indicating that the humid paleoclimate environment is more conducive to the enrichment of organic matter. The larger the C-value and CIA value are, the more humid the paleoclimate during the sedimentary period is, and the higher the organic matter content in the shale is.

The correlation coefficient  $R^2$  of the  $Xu5^1$  sub-member and the  $Xu5^2$  sub-member is significantly higher than that of the

other two sub-members, indicating that the paleoclimate during the sedimentary period of the Xu5¹ sub-member and the Xu5² sub-member has a stronger control effect on the enrichment of organic matter. The effect of paleosalinity on TOC was analyzed by the Sr/Ba ratio. As shown in Figure 11c, the Sr/Ba ratio is negatively correlated with TOC content as a whole, indicating that the environment with high salinity is more conducive to the enrichment of organic matter. When the salinity of the water body is high, it is easy to form salinity stratification, the convection of the water body is limited, and it is easy to form a reducing environment at the bottom of the water body, which is conducive to the enrichment of organic matter.

# 5.8 Effect of redox condition of bottom water on the enrichment of organic matter

The UEF and U/Th ratios were selected for analysis. The results showed that both of these two indicators were

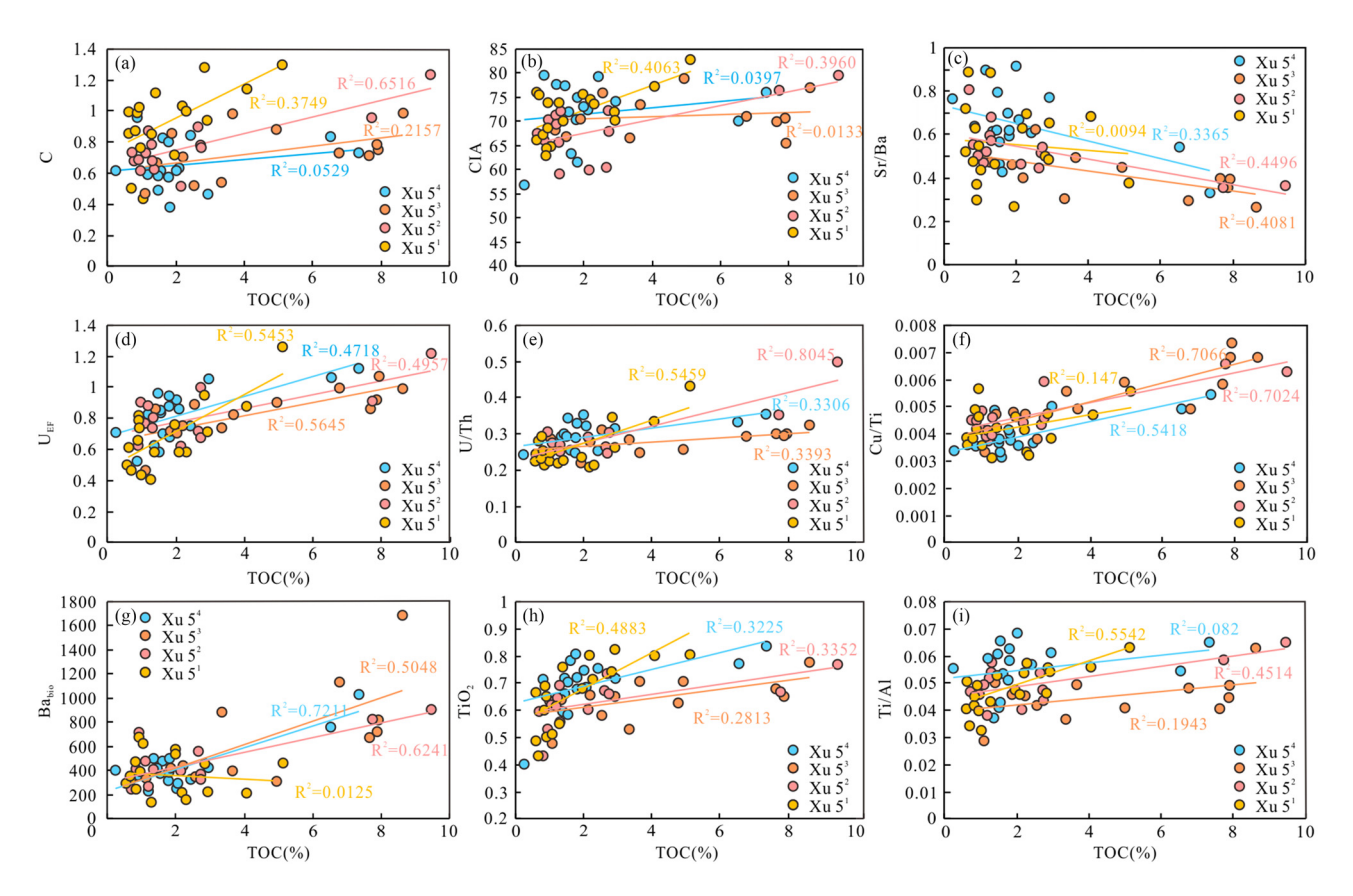


**Figure 11:** Relationship between paleoenvironmental indicators and organic matter enrichment in the fifth member of Xujiahe Formation. (a) crossplot of *C*-value and TOC; (b) crossplot of CIA and TOC; (c) the crossplot of Sr/Ba and TOC; (d) crossplot of UEF and TOC; (e) U/Th and TOC crossplot; (f) Cu/Ti and TOC crossplot; (g) Babio and TOC crossplot; and (h) crossplot of TiO<sub>2</sub> and TOC; and (i) intermember diagram of Ti/Al and TOC.

positively correlated with TOC content (Figure 11d and e), indicating that redox conditions had a significant effect on the enrichment of organic matter. The stronger the reduction of bottom water, the more conducive to the preservation of organic matter. The Cu/Ti ratio and Babio content were selected for the analysis of paleoproductivity indicators. The results showed that the Cu/Ti ratio and Babio content were positively correlated with TOC in the Xu5<sup>2</sup> to Xu5<sup>4</sup> sub-members, indicating that higher paleoproductivity can promote the enrichment of organic matter, and high paleobiological productivity will also lead to an increase in the amount of oxygen consumed by organisms, resulting in an increase in the reducibility of bottom water, which is more conducive to the preservation of organic matter. However, the correlation between paleoproductivity index and TOC in the first sub-member of Xujiahe Formation is poor, which may be due to the overall low level of paleoproductivity during this sedimentary period, which has little effect on the enrichment of organic matter. The effects of terrigenous debris input and deposition rate on the enrichment of organic matter.

The TiO<sub>2</sub> content and Ti/Al ratio were analyzed. As shown in Figure 11e and f, TiO2 and Ti/Al ratio were positively correlated with TOC, and the correlation between the Xu5<sup>1</sup> sub-member and the Xu5<sup>2</sup> sub-member was obvious due to the other two sub-members, indicating that the terrigenous input and deposition rate had a significant effect on the enrichment of organic matter during the deposition period of Xu5<sup>1</sup> to Xu5<sup>2</sup>. With the increase of the intensity of terrigenous debris input, more terrigenous nutrients entered the lake basin and were well preserved at a faster deposition rate, thus enriching organic matter. In summary, the enrichment degree of organic matter in Xu5<sup>1</sup> sub-member is mainly affected by paleoclimate, redox of bottom water, terrigenous clastic input, and deposition rate, and the enrichment degree of TOC is less affected by paleosalinity and paleoproductivity. The influencing factors of the enrichment degree of organic matter in the second member of Xujiahe Formation are basically the same as those in the first member of Xujiahe Formation, and the paleosalinity and paleoproductivity also have a good control effect on the enrichment degree of shale organic matter during the deposition period of the second member of Xujiahe Formation. The degree of organic matter enrichment of shale in the sedimentary period of Xu5<sup>3</sup>-Xu5<sup>4</sup> is mainly controlled by the redox conditions of bottom water, paleoproductivity, and paleosalinity, and the paleoclimate, terrestrial input intensity, and deposition rate have little effect on it.

Stratigraphically, the Xu5<sup>1</sup> to Xu5<sup>2</sup> sub-members were deposited under more humid paleoclimatic conditions

with higher precipitation, leading to stronger chemical weathering and greater terrestrial input(Figure 7). The increased flux of terrigenous detritus delivered more nutrients to the lacustrine system, while deeper water conditions and higher sedimentation rates promoted excellent organic matter preservation, resulting in significant OM enrichment. In the Xu5<sup>3</sup> to Xu5<sup>4</sup> interval, OM enrichment was primarily governed by bottom-water redox conditions, paleoproductivity, and paleosalinity. Upward-increasing C-values through Xu5<sup>3</sup> indicate progressively more humid conditions, decreasing salinity, and enhanced productivity, collectively driving TOC enrichment. During Xu5<sup>4</sup> deposition, increased aridity and evaporation elevated paleosalinity, creating favorable conditions for bottom-water OM preservation. However, the overall regressive trend from Xu5<sup>3</sup> to Xu5<sup>4</sup> led to reduced paleoproductivity and more oxic conditions, ultimately resulting in lower TOC contents in the Xu5<sup>4</sup> sub-member.

## 6 Conclusion

The shale of the fifth member of Xujiahe Formation in the Tianfu area predominantly comprises clay-rich and felsic lithofacies, exhibiting elevated TOC contents (average 3.71%) dominated by Type III kerogen with substantial hydrocarbon generation potential. Comparative analysis reveals significant vertical heterogeneity in organic richness: Member 3 shows the highest TOC values (1.09–8.63%), while Members 1, 2, and 4 display relatively lower organic contents (average 2%).

The shales of the fifth member of the Xujiahe Formation represent first-cycle deposits that underwent moderate chemical weathering, exhibiting high compositional maturity and significant terrigenous input. Provenance analysis indicates dominant felsic igneous sources with minor mafic contributions, deposited under relatively low sedimentation rates. Paleoenvironmental reconstruction reveals: (1) semi-humid to humid conditions during Xu5 Member deposition, with progressive aridification vertically through the stratigraphic column; (2) predominantly freshwater to brackish conditions; (3) generally oxic bottom waters with localized intervals of reduced conditions; and (4) variable paleoproductivity, peaking during the late Xu5<sup>3</sup> and early Xu5<sup>2</sup> submember intervals.

The Xujiahe Formation Member 5 exhibits distinct stratigraphic variability in primary controls on organic matter enrichment across its sub-members. In sub-member Xu5<sup>1</sup>, organic accumulation is principally governed by paleoclimatic conditions, bottom-water redox

state, terrigenous detrital flux, and sedimentation rate. Sub-members Xu5<sup>3</sup> and Xu5<sup>4</sup> demonstrate enrichment patterns primarily controlled by bottom-water redox conditions, paleoproductivity, and paleosalinity. Sub-member Xu5<sup>2</sup> displays more complex controls, with primary regulation by bottom-water redox, paleoproductivity, and paleosalinity, supplemented by secondary influences from paleoclimate, terrigenous input, and sedimentation rate.

**Acknowledgments:** Thank Professor Jiang Yuqiang for his guidance on this article, thank the editors for their work and efforts on this article, and thank the reviewers for their valuable comments on this article.

Funding information: This work was supported by the PetroChina Southwest Oil and Gas Field Branch Major Project (2022ZD01).

**Author contributions:** The order of authors of this article is as follows: Jian Yang, Yuqiang Jiang, Weihua Chen, Hui Pan, Xing Yang, Miao Li, Tao Liu, Zhanlei Wang, and Yifan Gu. Dr. Yang Jian completed the article conception, experimental data processing, and wrote the manuscript. Professor Yuqiang Jiang processed the experimental data and revised the manuscript. Dr. Weihua Chen, Hui Pan, and Xing Yang completed some experiments. Tao Liu, Zhanlei Wang, and Yifan Gu are responsible for sample preparation and article revision.

Conflict of interest: The authors state no conflict of interest.

Data availability statement: The data underlying this article will be shared on reasonable request to the corresponding author.

# References

- Pang XQ, Li M, Li BY, Wang T, Hui SS, Liu Y, et al. Main controlling factors and movability evaluation of continental shale oil. Earth-Sci Rev. 2023;243:104472.
- Ning ST, Xia P, Hao F, Tian JQ, Fu Y, Wang K. Pore fractal characteristics between marine and marine-continental transitional black shales: a case study of niutitang formation and longtan formation. Fractal Fract. 2024;8(5):288.
- Hu SY, Zhao WZ, Hou LH, Yang Z, Zhu RK, Wu ST, et al. Development potential and technical strategy of continental shale oil in China. Pet Explor Dev. 2020;47(4):877-87.
- Zhao WZ, Hu SY, Hou LH, Yang T, Li X, Guo BC, et al. Types and [4] resource potential of continental shale oil in China and its boundary with tight oil. Pet Explor Dev. 2020;47(1):1-11.

- Tang L, Song Y, Jiang ZX, Pang XQ, Li Z, Li QW, et al. Influencing factors and mathematical prediction of shale adsorbed gas content in the upper triassic yanchang formation in the ordos Basin, China. Minerals. 2019;9(5):265.
- Gao ZD, Wang YD, Gu XY, Cheng HL, Puppe N. Characteristics and gas-bearing properties of yanchang formation shale reservoirs in the Southern Ordos Basin. Geofluids. 2023;2023: 5894458.
- He WJ, Liu Y, Wang DX, Lei DW, Liu GD, Gao G, et al. Geochemical [7] Characteristics and Process of Hydrocarbon Generation Evolution of the Lucaogou Formation Shale, Jimsar Depression, Junggar Basin. Energies. 2022;15(7):2331.
- Zhao ZY, Lin SH, Luo X, Zhang LJ. Paleo-sedimentary environment and formation mechanism of the organic-rich shale of the permian lucaogou formation, Jimsar Sag, Junggar Basin, China. Minerals. 2024;14(7):635.
- Deng T, Li Y, Wang ZJ, Yu Q, Dong SL, Yan L, et al. Geochemical characteristics and organic matter enrichment mechanism of black shale in the Upper Triassic Xujiahe Formation in the Sichuan basin: Implications for paleoweathering, provenance and tectonic setting. Mar Pet Geol. 2019;109:698-716.
- Yu Y, Lin LB, Nan HL. Trace and rare-earth element characteristics [10] of fine-grained sediments in the Upper Triassic Xujiahe Formation in the western Sichuan Basin, SW China: implications for the provenance and depositional environment. Carbonates Evaporites.
- [11] Zhang R, Tang LX. Oil-bearing evaluation of different lithofacies in Da'anzhai Member, Central Sichuan Basin: implications for shale oil development. Pet Sci Technol. 2023;41(15):1477-91.
- Fang R, Jiang YQ, Luo Y, Wang ZL, Jiang C, Li S, et al. Hydrocarbon geological characteristics and factors controlling hydrocarbon accumulation of jurassic da'anzhai continental shale. Minerals. 2024;14(1):11.
- Γ131 Wu ZY, Zhao XZ, Wang EZ, Pu XG, Lash G, Han WZ, et al. Sedimentary environment and organic enrichment mechanisms of lacustrine shale: A case study of the Paleogene Shahejie Formation, Qikou Sag, Bohai Bay Basin. Palaeogeogr Palaeoclimatol Palaeoecol. 2021;573:110404.
- Bai J, Xu XY, Liu WB, Zhao WZ, Jiang H. Paleoenvironmental evolution and organic matter enrichment genesis of the late turonian black shale in the Southern Songliao Basin, NE China. Acta Geol Sin. 2024;98(5):1338-58.
- [15] Xu QL, Liu B, Ma YS, Song XM, Wang YJ, Chen ZX. Geological and geochemical characterization of lacustrine shale: A case study of the Jurassic Da'anzhai member shale in the central Sichuan Basin, southwest China. J Nat Gas Sci Eng. 2017;47:124-39.
- Zhang SH, Liu CY, Fan ZQ, Liang H, Gao JR, Song H, et al. Paleoenvironmental Conditions and Shale Oil Potential of the Carboniferous Ha'erjiawu Formation in the Santanghu Basin, NW China. Processes. 2023;11(7):2209.
- He QY, Li DL, Sun Q, Gao JW, Li HB, Li XH, et al. Constraints of palaeoenvironment on organic matter of Benxi Formation shale and discussion on enrichment mechanism under different facies. Front Earth Sci. 2023;18(1):148-71.
- [18] Du Y, Wang XZ, Zhao RR, Chen C, Wen SY, Tang RF, et al. Controlling factors of organic matter enrichment in continental shale: A case study of the Jurassic Da'anzhai member in the Sichuan Basin. Front Earth Sci. 2022;10:921529.
- Zhao YG, Zhang CY, Lu JG, Zhu XC, Li L, Si SH. Sedimentary environment and model for organic matter enrichment: Chang 7

- Shale of Late Triassic Yanchang Formation, Southern Margin of Ordos Basin, China. Energies. 2022;15(8):2948.
- [20] Wang YA, Cheng XL, Fan K, Huo ZP, Wei L. The Paleoenvironment and Mechanisms of Organic Matter Enrichment of Shale in the Permian Taiyuan and Shanxi Formations in the Southern North China Basin. J Mar Sci Eng. 2023;11(5):992.
- [21] Yin XD, Jiang S, Ma LT, Wu P. Paleoenvironment of the Upper Paleozoic marine-continental transitional shales and its implications for organic matter enrichment in the L-Block, eastern Ordos Basin, North China. Pet Sci Technol. 2022;40(5):519–33.
- [22] Zhao JH, Jin ZJ, Jin ZK, Geng YK, Wen X, Yan CN. Applying sedimentary geochemical proxies for paleoenvironment interpretation of organic-rich shale deposition in the Sichuan Basin. China. Int I Coal Geol. 2016:163:52–71.
- [23] Han SB, Du X, He YF, Wang CS, Huo MX, Mu XY, et al. Sedimentary paleoenvironment and organic matter enrichment characteristics of Lacustrine Shahezi Shale in Songliao Basin: insights from the continental scientific drilling. Acs Omega. 2024;9(19):21097–115.
- [24] Zhu F, Li CX, Leng JY, Jia MY, Gong HJ, Wang B, et al. Paleoenvironmental characteristics of lacustrine shale and its impact on organic matter enrichment in funing formation of Subei Basin. Minerals. 2024;13(11):1439.
- [25] Wei YB, Li XY, Zhang RF, Li XD, Lu SF, Qiu Y, et al. Influence of a paleosedimentary environment on shale oil enrichment: a case study on the shahejie formation of Raoyang Sag, Bohai Bay Basin, China. Front Earth Sci. 2021;9:736054.
- [26] Zhao BS, Li RX, Qin XL, Wang N, Zhou W, Khaled A, et al. Geochemical characteristics and mechanism of organic matter accumulation of marine-continental transitional shale of the lower permian Shanxi Formation, southeastern Ordos Basin, north China. J Pet Sci Eng. 2021;205:108815.
- [27] Chen ZP, Cui JP, Ren ZL, Jiang S, Liang X, Wang GC, et al. Geochemistry, Paleoenvironment and Mechanism of Organic-Matter Enrichment in the Lower Silurian Longmaxi Formation Shale in the Sichuan Basin, China. Acta Geol Sin. 2019;93(3):505–19.
- [28] Xiao B, Xiong L, Zhao ZY, Fu X, Zhao ZH, Hou HH, et al. Late Ordovician-Early Silurian extension of the northern margin of the Upper Yangtze Platform (South China) and its impact on organic matter accumulation. J Pet Sci Eng. 2023;220(A):111238.
- [29] Yu K, Ju YW, Wan ZJ, Zhao KD. Paleoenvironment, provenance, and hydrocarbon potential of lower permian coal-bearing source rocks in the Southern North China Basin: A case study of the pingdingshan coalfield. ACS Earth Space Chem. 2022;6(5):1299–310.
- [30] Wu Z, Shi JY, Fan TL, Jiang M. Sedimentary paleoenvironment and its control on organic matter enrichment in the Mesoproterozoic hydrocarbon source rocks in the Ordos Basin, southern margin of the North China Craton. Pet Sci. 2024;21(4):2257–72.
- [31] Xiao B, Guo DX, Li S, Xiong SZ, Jing ZY, Xiang F, et al. Rare Earth Element Characteristics of Shales from Wufeng–Longmaxi Formations in Deep-Buried Areas of the Northern Sichuan Basin, Southern China: Implications for Provenance, Depositional Conditions, and Paleoclimate. ACS Omega. 2024;9:2088–103.
- [32] Huang JL, Zou CN, Dong DZ, Li JZ, Wang YM, Wang SJ, et al. Geochemical and reservoir characteristics of the Upper Triassic continental shale in the Sichuan Basin, China. Energy Explor Exploit. 2015;33(3):375–95.
- [33] Dong L, Bian CS, Guo BC, Zeng X, Liang S. Pore structure and reservoir physical properties for effective development of tight

- sandstone gas: A case study from the Central Sichuan Basin, China. Geol J. 2022;57(7):2497–510.
- [34] Feng LJ, Jiang YQ, Guo GA, Yang CC, Zhu X, Zeng QG, et al. Pore structure and fractal characteristics of tight sandstone in meandering stream facies: a case study of the J2s2 member in the central Sichuan Basin, China. Front Earth Sci. 2023;11:1183734.
- [35] Lai J, Wang GW, Ran Y, Zhou ZL. Predictive distribution of high-quality reservoirs of tight gas sandstones by linking diagenesis to depositional facies: Evidence from Xu-2 sandstones in the Penglai area of the central Sichuan basin, China. J Nat Gas Sci Eng. 2015;23:97–111.
- [36] Wu ZJ, Li TF, Ji S, Zhou Q, Tian H. Gas generation from coal and coalmeasure mudstone source rocks of the xujiahe formation in the western Sichuan Depression, Sichuan Basin. J Earth Sci. 2023;34(4):1012–25.
- [37] Wang ZH, Hao CG, Jin H, Cun JF, Wu XQ, Bo DM, et al. Geochemical characteristics and hydrocarbon generation potential of main source rocks in the Upper Triassic Xujiahe Formation, Sichuan Basin, China. Front Earth Sci. 2023;11:1233959.
- [38] Xu K, Chen SJ, Lu JG, Li Y, Zhu XC, Liu JH, et al. Palaeosedimentary Environment and Formation Mechanism of High-Quality Xujiahe Source Rocks, Sichuan Basin, South China. Lithosphere. 2022;2022(13):7185107.
- [39] Xie ZY, Li J, Li ZS, Guo JY, Li J, Zhang L, et al. Geochemical characteristics of the upper triassic xujiahe formation in sichuan basin, china and its significance for hydrocarbon accumulation. Acta Geol Sin. 2017;91(5):1836–54.
- [40] Zhang L, Guo XS, Hao F, Zou HY, Li PP. Lithologic characteristics and diagenesis of the Upper Triassic Xujiahe Formation, Yuanba area, northeastern Sichuan Basin. J Nat Gas Sci Eng. 2016;35:1320–35.
- [41] Jiang L, Zhao W, Bo DM, Fan Y, Zhou G, Hao JQ. Densification mechanism and natural gas accumulation process, triassic xujiahe formation, Hechuan Area, Sichuan Basin, China. Lithosphere. 2022;2022(13):4522740.
- [42] Zhao ZY, Zhao JH, Wang HJ, Liao JD, Liu CM. Distribution and application of trace elements in Junggar Basin [in Chinese with English abstract. Nat Gas Explor Dev. 2007;30(2):4.
- [43] Li Q, Wu SH, Xia DL, You XL, Zhang HM, Lu H. Major and trace element geochemistry of the lacustrine organic-rich shales from the Upper Triassic Chang 7 Member in the southwestern Ordos Basin, China: Implications for paleoenvironment and organic matter accumulation. Mar Pet Geol. 2020;111:852–67.
- [44] Nesbitt HW, Young GM. Early Proterozoic climates and plate motions inferred from major element chemistry of lutites. Nature. 1982;299(5885):715–7.
- [45] Garzanti E, Padoan M, Andò S, Resentini A, Vezzoli G, Lustrino M. Weathering and relative durability of detrital minerals in equatorial climate: Sand petrology and geochemistry in the East African Rift. J Geol. 2013;121(6):547–80.
- [46] Wedepohl KH. The composition of the continental crust. Geochim Cosmochim Acta. 1995;59(7):1217–32.
- [47] Ma K, Hu SY, Wang TS, Zhang BM, Qin SF, Shi SY, et al. Sedimentary environments and mechanisms of organic matter enrichment in the Mesoproterozoic Hongshuizhuang Formation of northern China. Palaeogeogr, Palaeoclimatol, Palaeoecol. 2017;75:176–87.
- [48] Taylor S, McLennan S. The continental crust, its composition and evolution. Vol. 312, New Jersey: Blackwell Scientific Publications; 1985.
- [49] Hu ZC, Gao S. Upper crustal abundances of trace elements, A revision and update. Chem Geol. 2008;253:205–21.

- [50] Qiu XW, Liu CY, Wang FF, Deng Y, Mao GZ. Trace and rare earth element geochemistry of the Upper Triassic mudstones in the southern Ordos Basin, Central China. Geol J. 2015;50(4):399-413.
- [51] Wu ZY, Zhao XZ, Li JZ, Pu XG, Tao XW, Shi ZN, et al. Paleoenvironmental modes and organic matter enrichment mechanisms of lacustrine shale in the Paleogene Shahejie Formation, Qikou Sag, Bohai Bay Basin. Energy Rep. 2021;7:9046-68.
- [52] Cox R. Lowe DR. Cullers RL. The influence of sediment recycling and basement composition on evolution of mudrock chemistry in the southwestern United States. Geochim Cosmochim Acta. 1995;59(14):2919-40.
- [53] Yan DT, Chen DZ, Wang QC, Wang JG. Large-scale climatic fluctuations in the latest Ordovician on the Yangtze block, south China. Geology. 2010;38(7):599-602.
- [54] Tang L, Song Y, Pang X, Jiang Z, Guo Y, Zhang H, et al. Effects of paleo sedimentary environment in saline lacustrine basin on OM accumulation and preservation: a case study from the Dongpu Depression, Bohai Bay Basin, China. | Pet Sci Eng. 2020;185:106669.
- [55] Meng Q, Liu Z, Bruch AA, Liu R, Hu F. Palaeoclimatic evolution during Eocene and its influence on oil shale mineralisation, Fushun basin, China. | Asian Earth Sci. 2012;45:95-105.
- [56] Algeo TJ, Maynard JB. Trace-element behavior and redox facies in core shales of Upper Pennsylvanian Kansas-type cyclothems. Chem Geol. 2004;206(3-4):289-318.
- [57] Tribovillard N, Algeo TJ, Lyons T, Riboulleau A. Trace metals as paleoredox and paleoproductivity proxies: an update. Chem Geol. 2006;232:12-32.
- [58] Zhang S, Liu C, Liang H, Wang J, Bai J, Yang M, et al. Paleoenvironmental conditions, OM accumulation, and unconventional hydrocarbon potential for the Permian Lucaogou Formation organic-rich rocks in Santanghu Basin, NW China. Int J Coal Geol. 2018;185:44-60.

- [59] Pan Y, Huang Z, Li T, Guo X, Xu X, Chen X. Environmental response to volcanic activity and its effect on OM enrichment in the Permian Lucaogou Formation of the Malang Sag, Santanghu basin, northwest China. Palaeogeogr Palaeoclimatol Palaeoecol. 2020;560:110024.
- [60] Algeo TJ, Ingall E. Sedimentary Corg: P ratios, paleocean ventilation, and Phanerozoic atmospheric pO2. Palaeogeogr, Palaeoclimatol, Palaeoecol. 2007;256:130-55.
- Г**6**11 Fathy D. Wagreich M. Gier S. Mohamed RSA. Zaki R. El Nady MM. Maastrichtian oil shale deposition on the southern Tethys margin, Egypt: Insights into greenhouse climate and paleoceanography. Palaeogeogr, Palaeoclimatol, Palaeoecol. 2018;505:18-32.
- [62] Ingall E, Jahnke R. Evidence for enhanced phosphorus regeneration from marine sediments overlain by oxygen depleted waters. Geochim Cosmochim Acta. 1994:58(11):2571-5.
- [63] Kidder DL, Erwin DH. Secular distribution of biogenic silica through the Phanerozoic: comparison of silica-replaced fossils and bedded cherts at the series level. J Geol. 2001;109(4):509-22.
- [64] Hayashi KI, Fujisawa H, Holland HD, Ohmoto H. Geochemistry of 1.9 Ga sedimentary rocks from northeastern Labrador, Canada. Geochim Cosmochim Acta. 1997;61(19):4115-37.
- [65] Tyson RV. Sedimentation rate, dilution, preservation and total organic carbon: some results of a modelling study. Org Geochem. 2001;32(2):333-9.
- Chen YH, Wang YB, Guo MQ, Wu HY, Li J, Wu WT, et al. Differential [66] enrichment mechanism of organic matters in the marinecontinental transitional shale in northeastern Ordos Basin, China: Control of sedimentary environments. J Nat Gas Sci Eng. 2022;83:103625.
- [67] Shi J, Zou YR, Cai YL, Zhan ZW, Sun JN, Liang T, et al. Organic matter enrichment of the Chang 7 member in the Ordos Basin: Insights from chemometrics and element geochemistry. Mar Pet Geol. 2022;135:105404.